Programmed cell death in bacteria: translational repression by mRNA end-pairing

Thomas Franch and Kenn Gerdes*
Department of Molecular Biology, Odense University, DK-5230, Odense M, Denmark.

Summary

The *hok/sok* and *pnd* systems of plasmids R1 and R483 mediate plasmid maintenance by killing plasmid-free cells. Translation of the exceptionally stable *hok* and *pnd* mRNAs is repressed by unstable antisense RNAs. The different stabilities of the killer mRNAs and their cognate repressors explain the onset of translation in plasmid-free cells. The full-length *hok* and *pnd* mRNAs are inert with respect to translation and antisense RNA binding. We have previously shown that the mRNAs contain two negative translational control elements. Thus, the mRNAs contain upstream anti-Shine–Dalgarno elements that repress translation by shielding the Shine–Dalgarno elements. The mRNAs also contain fold-back-inhibition elements (*fbi*) at their 3' ends that are required to maintain the inert mRNA configuration. Using genetic complementation, we show that the 3' *fbi* elements pair with the very 5' ends of the mRNAs. This pairing sets the low rate of 3' exonucleolytical processing, which is required for the accumulation of an activatable pool of mRNA. Unexpectedly, the *hok* and *pnd* mRNAs were found to contain translational activators at their 5' ends (termed *tac*). Thus, the *fbi* elements inhibit translation of the full-length mRNAs by sequestration of the *tac* elements. The *fbi* elements are removed by 3' exonucleolytical processing. Mutational analyses indicate that the 3' processing triggers refolding of the mRNA 5' ends into translatable configurations in which the 5' *tac* elements base pair with the anti-Shine–Dalgarno sequences.

Introduction

Translational control of gene expression in prokaryotes has been extensively studied (reviewed by Gold, 1988; McCarthy and Gualerzi, 1990; McCarthy and Brimacombe, 1994). Translational control is usually negative.

The negative control elements can be divided into three main categories: *trans*-acting proteins, *trans*-acting RNAs (called antisense RNAs), and *cis*-acting elements in the mRNAs. Typically, protein repressors bind and sequester an essential part of a translational initiation region. Antisense RNAs inhibit target RNA function by a number of different mechanisms, including direct sequestration of a translation initiation region, accelerated mRNA decay, target RNA refolding, and even transcriptional attenuation (reviewed by Wagner and Simons, 1994; Eguchi et al., 1991). However, the most common theme of negative translational control involves the formation of RNA secondary structures that sequester an essential part of a translation initiation region. Usually, such sequestration involves local folding of the Shine–Dalgarno (SD) regions into stable stem-loop structures (de Smit and van Duin, 1990), but in some cases long-range RNA–RNA interactions are implicated (Saito and Richardson, 1981; Petersen, 1989).

The *hok/sok* and *pnd* systems of plasmids R1 and R483 belong to a family of homologous gene systems that mediate plasmid maintenance by killing of plasmid-free segregants (Gerdes et al., 1986a; 1990a). These loci encode highly stable mRNAs that can be translated into toxic membrane proteins (Hok and PndA) which kill the cells from within (Gerdes et al., 1986b). Translation of *hok* and *pndA* is regulated by small unstable antisense RNAs, the Sok and PndB RNAs, that are complementary to the leader regions of the *hok* and *pnd* mRNAs (Gerdes et al., 1990b; Nielsen et al., 1991). The antisense RNAs inhibit translation of reading frames that overlap with the toxin-encoding genes (*mok* and *pndC*, see Fig. 1). As translation of *hok* and *pndA* is coupled to that of *mok* and *pndC*, respectively, the antisense RNAs inhibit *hok* and *pndA* translation indirectly (Thisted and Gerdes, 1992).

The *hok* (host killing) gene family now consists of nine homologous systems, five of which were isolated from *Escherichia coli* plasmids: *hok/sok* from R1, *flm* and *srnB* from F, and *pnd* from R483 and R16 (Gerdes et al., 1990a). The *E. coli* chromosome encodes at least three different *hok*-homologous genes (Gerdes et al., 1986b; Poulsen et al., 1991; K. Pedersen and K. Gerdes, unpublished). Recently, we identified a new *hok*-homologous gene encoded by the chromosome of the enteric bacterium *Hafnia alvei* (K. Gerdes, unpublished). All of the plasmid-encoded systems mediate plasmid maintenance by killing of plasmid-free segregants. These systems are

A   *hok/sok* of Plasmid R1


B   *pnd* of Plasmid R483
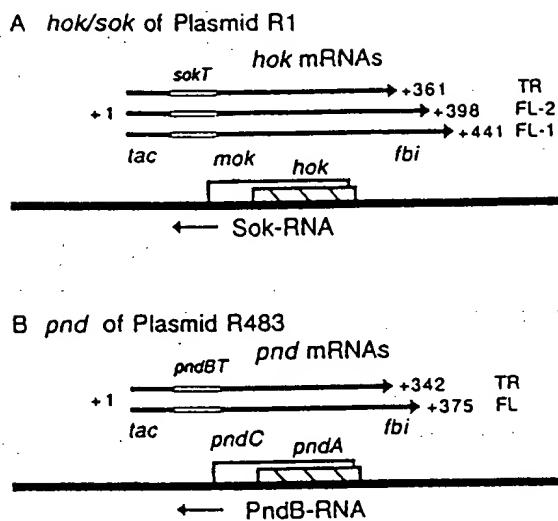
Fig. 1. Genetic organization and RNAs of the killer gene systems *hok/sok* of R1 and *pnd* of R483. Arrows indicate the RNAs encoded by the systems. Cross-hatched boxes indicate the *hok* and *pndA* genes, and open boxes indicate the *mok* and *pndC* reading frames. Genetic nomenclature: *hok*: host killing; *sok*: suppression of killing; *mok*: modulator of killing; *pnd*: promotion of nucleic acid degradation; *fbi*: fold-back-inhibitory elements; *tac*: translational activator elements; *sokT*: Sok target region; *pndBT*: PndB target region. The 3' end is at +441 in full-length *hok* mRNA-1, at +398 in full-length *hok* mRNA-2, and at +361 in truncated *hok* mRNA. Full-length *pnd* mRNA has the 3' end at +375, whereas it is at +342 in truncated *pnd* mRNA. FL denotes full-length mRNAs; TR denotes truncated mRNAs.

also induced by the addition of the transcriptional inhibitor rifampicin to growing cells (Gerdes *et al.*, 1990b; Nielsen *et al.*, 1991). The *hok*-like genes located on bacterial chromosomes do not mediate post-segregational killing, and their function is not yet understood.

The killing of plasmid-free cells and the induction by rifampicin rely on the differential-decay rates of the toxin-producing mRNAs and the inhibitory antisense RNAs: plasmid-free segregants or cells treated with rifampicin experience a rapid decay of the antisense RNAs. Consequently, in these cells, an uninhibited pool of stable mRNA can be translated into the cytotoxins (Gerdes *et al.*, 1988). As such, plasmid loss can be regarded as a differentiation event that initiates a program eventually leading to cell death. One problem of the proposed scheme is, however, that it fails to explain how the killer mRNAs circumvent irreversible inactivation by the antisense RNAs in plasmid-carrying cells, as antisense RNA binding leads to duplex formation, followed by rapid RNase III cleavage and irreversible mRNA decay (Gerdes *et al.*, 1992). The complex mechanism by which the killer mRNAs avoid irreversible inactivation has attracted considerable interest and is outlined below.

Two full-length *hok* mRNAs (termed *hok* mRNA-1 and -2) and one full-length *pnd* mRNA are present in plasmid-carrying cells (see Fig. 1). Full-length *hok* mRNA-2 is generated from mRNA-1 by RNase III cleavage (Gerdes

et al., 1992). The full-length mRNAs are translationally inactive and bind their cognate antisense RNAs inefficiently (Gerdes *et al.*, 1990b; Nielsen *et al.*, 1991; Thisted *et al.*, 1994a; T. Franch, unpublished). Translation of the full-length mRNAs is activated by slow 3'-end exonucleolytical processing by polynucleotide phosphorylase and ribonuclease II (N. Dam Mikkelsen, unpublished). Thus, plasmid-free cells inherit a pool of inert full-length killer mRNA that is activated by the removal of inhibitory elements located at the mRNA 3' ends. After decay of the antisense RNAs, the 3' processing leads to accumulation of truncated, translatable *hok* and *pnd* mRNAs, and killing of the plasmid-free cells ensues. In contrast, in plasmid-carrying cells, the truncated mRNAs are rapidly bound by the antisense RNAs, and the resulting RNA duplexes are destabilized by RNase III cleavage (Gerdes *et al.*, 1992). Hence, the truncated mRNAs are not present in detectable amounts in growing cells (Gerdes *et al.*, 1990b). In accordance with the above scheme, addition of rifampicin to growing cells leads to antisense RNA depletion, followed by accumulation of the truncated, translatable mRNAs. In turn, this leads to synthesis of the cytotoxins Hok and PndA.

The inhibitory elements in the 3' ends of *hok* and *pnd* mRNAs were termed *fbi* (fold-back inhibition; Thisted *et al.*, 1994a; Nielsen and Gerdes, 1995). Structural analysis of the entire full-length *hok* mRNA suggested that the *fbi* element pairs with the SD sequence of *mok* (Thisted *et al.*, 1995). However, a genetic analysis failed to confirm the presence of a similar structure in the *pnd* mRNA (Nielsen and Gerdes, 1995). On the contrary, this analysis indicated that the *pndC* SD is sequestered by a local secondary structure. Thus, in addition to the inhibitory *fbi* elements at their 3'-ends, the killer mRNAs also contain upstream anti-SD elements.

Using a genetic approach, we show that the *fbi* elements in the 3' ends of the *hok* and *pnd* mRNAs pair with the very 5' ends of the mRNAs. Surprisingly, the *hok* and *pnd* mRNAs were found to contain translational activator elements (*tac*) in their very 5' ends approx. 100 nucleotides (nt) upstream of the translation initiation regions. Thus, the 3' *fbi* elements repress translation by sequestration of the 5' *tac* elements. Mutational analyses indicate that the 3'-end processing triggers refolding of the mRNA 5' ends into translatable configurations in which the *tac* elements are base paired with the anti-SD sequences.

Results

Mutations in the 3' *fbi* elements of the hok and pnd mRNAs increase 3' processing and inactivate post-segregational killing

Recently, we found that mutations in the *fbi* motif in the *pnd* mRNA of plasmid R483 dramatically increase the processing rate at its 3' end (Nielsen and Gerdes, 1995). In this
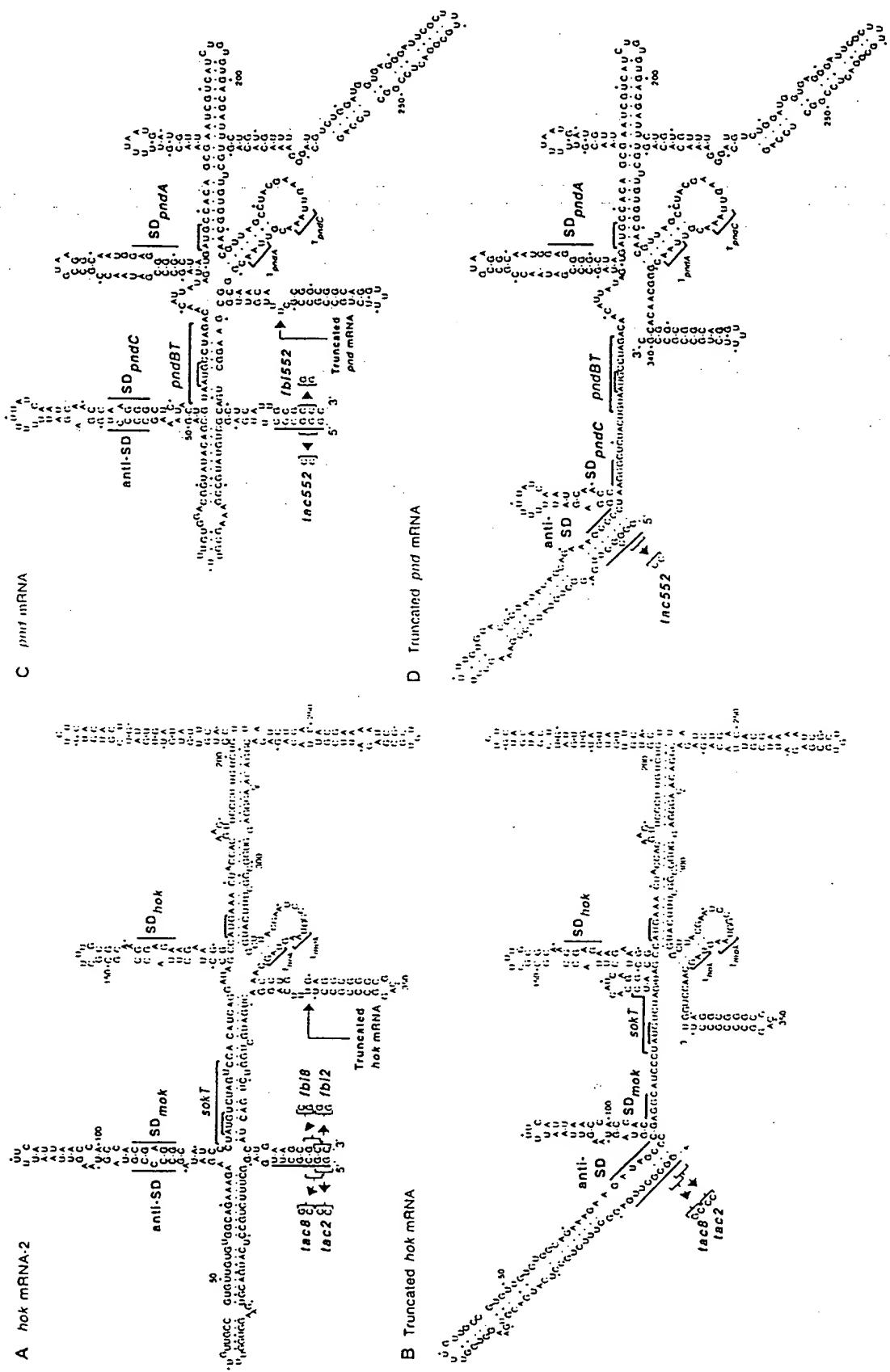
Fig. 2. Proposed secondary structures of the entire full-length and truncated *hok* and *pnd* mRNAs. SD, Shine–Dalgarno elements; anti-SD, elements sequestering SD elements; *tac*, translational activator elements; *fbi*, fold-back-inhibitory elements; T$_{hok}$ and T$_{mok}$, termination codons of *hok* and *mok*; T$_{pndA}$ and T$_{pndC}$, termination codons of *pndA* and *pndC*; *sokT* and *pndBT*, primary recognition elements of the Sok and PndB antisense RNAs.
A. Full-length *hok* mRNA.
B. Truncated *hok* mRNA.
C. Full-length *pnd* mRNA.
D. Truncated *pnd* mRNA.

a.

b.

c.
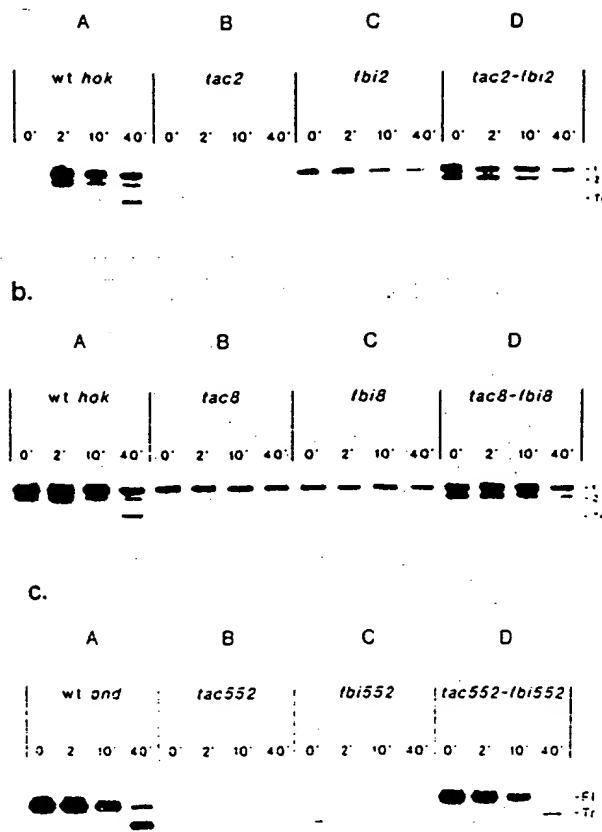
Fig. 3. *In vivo* processing patterns of wt and mutated *hok* and *pnd* mRNAs.
a. Northern analysis showing the effects of the *tac2* and *fbi2* mutations in *hok* mRNA.
b. Effects of the *tac8* and *fbi8* mutations in *hok* mRNA.
c. Effects of the *tac552* and *fbi552* mutations in *pnd* mRNA.
Panels: A. wt mRNAs; B. *tac* mutations; C. *fbi* mutations; D. *tac-fbi* double mutations. Time points of sampling relative to the addition of rifampicin (at time zero) are indicated above each lane. The positions of *hok* mRNA-1. *hok* mRNA-2 and truncated *hok* mRNA are indicated with 1, 2. and Tr. respectively. Fl. denotes full-length *pnd* mRNA. The experiment was performed using the rifampicin-permeable strain AS19 carrying the wt and mutated killer gene systems cloned in pBR322.

study, we introduced mutations at similar locations in the *fbi* motif in the 3′ end of the *hok* mRNA (*fbi2* and *fbi8* in Fig. 2A). Their effect on *hok* mRNA processing and stability was investigated using Northern analysis. As seen in Fig. 3, a and b, panel C, the *fbi2* and *fbi8* mutations have a dramatic effect on the processing pattern of *hok* mRNA. Both mutations caused a disappearance of full-length *hok* mRNA-2, and truncated *hok* mRNA did not appear after addition of rifampicin. The amount of full-length *hok* mRNA-1 was also significantly reduced. The *fbi552* mutation in the *pnd* mRNA had a similar, but even more dramatic effect (Fig. 3c, panel C). The observed *in vivo* effects of the *fbi* mutations indicate that they cause an increased processing rate from full-length to truncated mRNAs.

To directly test this inference, full-length *hok* and *pnd* mRNAs and their mutated variants were synthesized *in vitro* and processing was investigated in a cell-free S30 extract. As seen in Fig. 4a, the *fbi2* mutation in the *hok* mRNA caused a highly increased processing rate from full-length to truncated mRNA (cf. panels A and C), as did the *fbi552* mutation in the *pnd* mRNA (cf. panels A and C in Fig. 4b). These results indicate that the low abundance, *in vivo*, of the full-length *hok* and *pnd* mRNAs carrying the *fbi* mutations is due to highly increased processing rates at their 3′ ends.

The wild-type (wt) *hok/sok* and *pnd* systems mediate an approx. 100-fold stabilization of mini-R1 plasmids by killing of plasmid-free segregants (Gerdes *et al.*, 1985; Nielsen *et al.*, 1991). We tested whether the *hok/sok* and *pnd* systems carrying the *fbi* mutations could stabilize a mini-R1 test plasmid (pOU82). Table 1 shows that *fbi2* and *fbi8* in *hok/sok* and *fbi552* in *pnd* completely inactivated the post-segregational killing effect, consistent with the absence of truncated. active killer mRNAs after addition of rifampicin (Fig. 3, panels C).

Mutations in the 5′ tac elements of the hok and pnd mRNAs also enhance 3′ processing and inactivate post-segregational killing

Mutations were introduced into the extreme 5′ ends of

a.
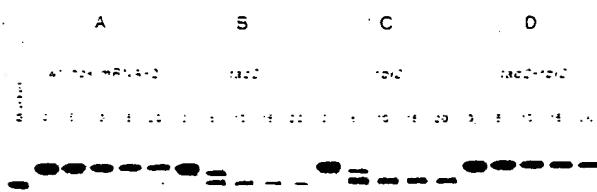
b.
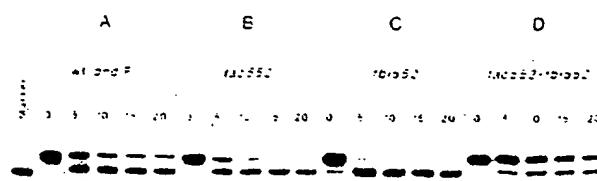
Fig. 4. *In vitro* processing patterns of wt and mutated *hok* and *pnd* mRNAs showing the *tac–fbi* interaction. Purified, uniformly ^{32}P-labelled full-length mRNAs were exposed to a cell-free S30 extract for the periods indicated above each lane.
a. *hok* mRNA-2.
b. Full-length (Fl.) *pnd* mRNA.
Panels: A. wt mRNAs; B. *tac2* and *tac552*; C. *fbi2* and *fbi552*; D. *tac2-fbi2* and *tac552-fbi552* double mutations. The marker lanes contained *in vitro* synthesized truncated *hok* and *pnd* mRNAs. respectively.

Table 1. Effects of *fbi* and *tac* mutations on post-segregational killing.

Plasmid	Killer system present	Mutation(s) present	LF value (loss-frequency cell^{-1} gen^{-1} x 10^{-4})	Folds of stabilization
pOU82(vector)[a]	None	–	200	1
pTT820	*hok/sok*	wt	2	100
PTF840	*hok/sok*	*tac2*	200	1
pTF841	*hok/sok*	*fbi2*	200	1
pTF842	*hok/sok*	*tac2, fbi2*	60	3
pTF850	*hok/sok*	*tac8*	200	1
PTF851	*hok/sok*	*fbi8*	200	1
pTF852	*hok/sok*	*tac8, fbi8*	7	30
pAN3	*pnd*	wt	2	100
pAN141	*pnd*	*fbi552*	200	1
pKG860	*pnd*	*tac552*	200	1
pKG862	*pnd*	*tac552, fbi552*	200	1

a. pOU82 is a *lacZYA*-carrying vector of 12 594 nucleotides derived from plasmid R1.

the *hok* and *pnd* mRNAs (see Fig. 2). These mutations were named translational activator or *tac*. The *in vivo* effect of the *tac2* and *tac8* mutations on the *hok* mRNA band pattern is shown in Fig. 3. a and b (panel B). Full-length *hok* mRNA-2 was not detected even before the addition of rifampicin, and the amount of full-length *hok* mRNA-1 was reduced. The *tac552* mutation in the *pnd* system had an even more dramatic effect: mutated, full-length *pnd* mRNA was only barely detectable after prolonged exposure of the autoradiogram (Fig. 3c. panel B).

The effect of the *tac* mutations on mRNA processing *in vitro* was also investigated. As seen from Fig. 4, a and b. the *tac* mutations resulted in rapid processing of full-length to truncated *hok* and *pnd* mRNAs (cf. panels A and B).

Finally, the effect of the *tac* mutations on post-segregational killing was investigated (Table 1): all these mutations resulted in inactivation of post-segregational killing. consistent with the absence of the respective truncated effector mRNAs (Fig. 3).

In conclusion, the effects of the *tac* mutations were identical to those of the *fbi* mutations. This coincidence urged us to investigate whether the opposite ends of the *hok* and *pnd* mRNAs might interact.

The extreme ends of the hok and pnd mRNAs pair

The *tac* mutations described above were designed such that the potential base pairing between the 3' and 5' ends of the mRNAs would be restored in the double *tac–fbi* mutants (see Fig. 2, A and C). Therefore, in *hok/sok*, *fbi2* was combined with *tac2*, and *fbi8* was combined with *tac8*. Similarly, in *pnd*, *fbi552* was combined with *tac552*. The *in vivo* RNA band patterns of the double mutants are shown in panels D of Fig. 3. This shows that the processing patterns of the doubly mutated mRNAs resembled that of the wt mRNAs in all cases. Similarly, the *in vitro* assay indicated that the *tac* mutations counteracted the effect of the *fbi* mutations on the RNA processing pattern (Fig. 4, panels D).

These combined *in vivo* and *in vitro* results yield strong genetic evidence that the very 3' ends of the *hok* and *pnd* mRNAs pair with their very 5' ends, and that this interaction is required for the characteristic processing patterns of the RNAs. These results are incorporated into the secondary structure models of the full-length *hok* and *pnd* mRNAs as presented in Fig. 2, A and C (see the *Discussion*). Our observations further indicate that the secondary structures of the full-length *hok* and *pnd* mRNAs synthesized *in vitro* very closely resemble those of the mRNAs produced *in vivo*, at least with respect to the long-range end-pairing.

The tac mutations do not suppress the fbi mutations at the functional level

The effect on post-segregational killing of the combination of the *tac* and *fbi* mutations was tested. As seen in Table 1, *tac552* did not suppress *fbi552* at the functional level, i.e. the *pnd* system carrying the *tac552, fbi552* double mutation did not exert post-segregational killing. In *hok/sok*, *tac2* and *tac8* only partially suppressed *fbi2* and *fbi8*, respectively. These results were unexpected, as the doubly mutated *hok* and *pnd* mRNAs exhibited wt *in vivo* and *in vitro* processing patterns (Figs 3 and 4). One explanation for this could be that the *tac* mutations prevented translation of the truncated *hok* and *pnd* mRNAs.

Mutations in the tac elements impair translation

In vitro generated truncated *hok* and *pnd* mRNAs were translated in the S30 extract used above (Zubay, 1973; see the *Experimental procedures* for details). Figure 5 shows that truncated wild type *hok* and *pnd* mRNAs were translated efficiently. Surprisingly, however, the *tac552* mutation abolished translation of the *pnd* mRNA, and the *tac2* mutation severely reduced translation of the *hok* mRNA. The *tac8* mutation also reduced *hok* mRNA
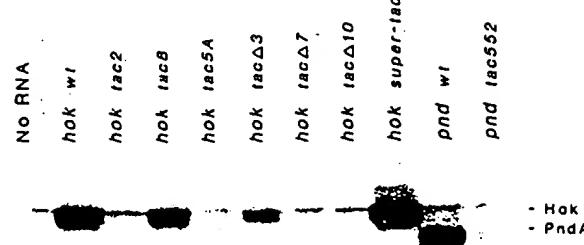
Fig. 5. *In vitro* translation of truncated wt and mutated *hok* and *pnd* mRNAs. Autoradiograph of *in vitro* translation reactions labelled with [³⁵S]-methionine and fractionated by SDS–PAGE. The positions of the Hok and PndA proteins are indicated. The type of mRNA added is indicated above each lane. The base changes of the *tac* and *fbi* mutations are shown in Fig. 6. A total of 3.0 pmol of template mRNA was added to each translation reaction.

translation to some extent. The translation rates of the mutated mRNAs were quantified and are shown in Fig. 6. Low translation yields were not due to instability of the mutated mRNAs in the extract (see Fig. 4). The absence of post-segregational killing *in vivo* (Table 1) is consistent with the reduced *in vitro* translation rates of the mutated *hok* and *pnd* mRNAs. These observations indicate that the extreme 5′ ends of the *hok* and *pnd* mRNAs contain elements required for their efficient translation. We denote these sequences as translational activator elements (*tac*).

Mutational analysis of the tac elements

To obtain a more-precise genetic definition of the *tac* elements, we introduced a number of deletions and substitutions in the extreme 5′ end of the *hok* mRNA (Fig. 6). The mutations were designed to reduce or abolish the proposed interaction between *tac* and the anti-SD element (see the *Discussion*). The effect of these mutational changes on the proposed secondary structure of the *tac* stem is also shown in Fig. 6. Messenger RNAs carrying the various *tac* mutations were synthesized *in vitro* and translated in an S30 cell-free extract. As shown in Fig. 6, deletion of the three 5′ nucleotides (*tacΔ3* mRNA) resulted in a severely reduced translation rate, and deletion of seven and 10 nucleotides abolished translation (*tacΔ7* and *tacΔ10* mRNAs).

In principle, the low translation rates of the mRNAs carrying the deletions could be due to the lack of the nucleotides *per se*. Therefore, the nucleotides from +2 to +6 were substituted with 5 rA's, resulting in the *tac5A* mRNA. As indicated in Fig. 6, this substitution abolished translation, as in the case of the deletions. These results verify that translation of the *hok* mRNAs is dependent on the nucleotides from +1 to +7, the translational activator sequence (*tac*).

Introduction of a perfect tac stem leads to super translation

The refolding model states that the *tac* anti-SD interaction is required for activation of translation. The above mutational analysis is consistent with the refolding model. To obtain more solid evidence for the postulated mechanism, we constructed a truncated *hok* mRNA with a 'perfect' *tac* stem. The proposed secondary structure of the 5′ end of
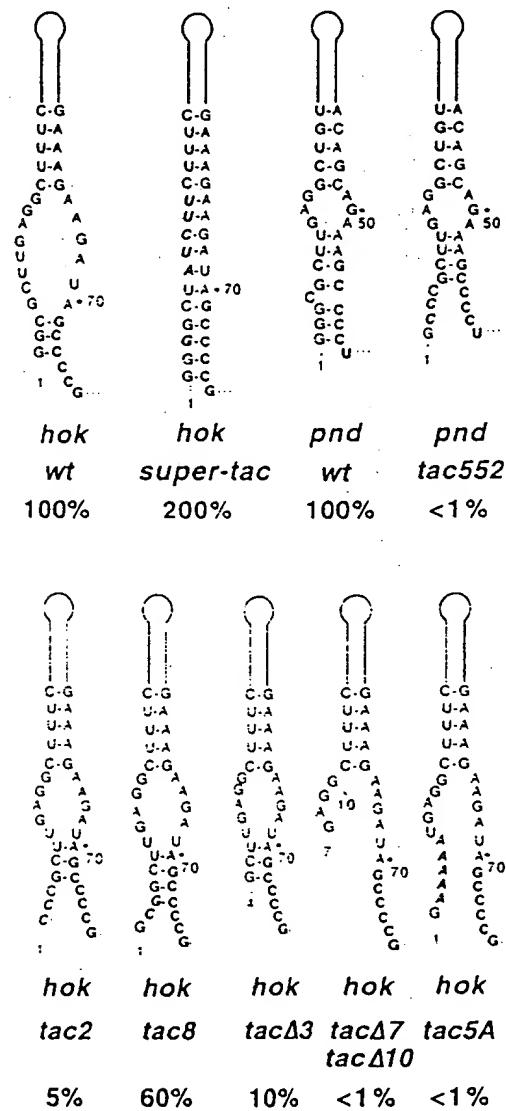

Fig. 6. Primary and proposed secondary structures of wt and mutated translational activator stems (*tac*). The upper row shows the *tac* stems of the wt *hok*, super-*tac* in *hok*, the wt *pnd* system and *pnd* carrying the *tac552* mutation. The lower row shows mutated *tac* stems in *hok* mRNA. Anti-SD elements are shown in bold, and mutated bases are shown in bold italic. 1 denotes the mRNA 5′ ends. The percentages indicate the degree of translatability for each mRNA as determined by the *in vitro* translation assay (see Fig. 5) and were obtained using a PhosphorImager (Molecular Dynamics). The translatability of wt *hok* and *pnd* mRNAs was set at 100%.

this mutated mRNA is also shown in Fig. 6 (the 'super-*tac*' mutation). As seen in Fig. 6, the translation rate of the mRNA carrying the super-*tac* mutation was twofold that of the wt truncated *hok* mRNA. As the super-*tac* mRNA was destabilized in the S30 extract, the translation rate obtained was a lower estimate. Thus, the presence of the super-*tac* mutation leads to a significant increase in the translatability of the *hok* mRNA. This result lends further support to the hypothesis that activation of translation is a consequence of the proposed interaction between *tac* and the anti-SD element.

Discussion

The folded structures of the full-length hok and pnd mRNAs

Recently, we analysed the secondary structure of the entire full-length *hok* mRNA (Thisted *et al.*, 1994a; 1995). These analyses suggested that the extreme 3' end of the full-length *hok* mRNA folds back onto the *mok* SD region, thus preventing ribosome binding and, therefore, translation. However, a mutational analysis of the *pnd* mRNA failed to confirm the presence of a similar *fbi* structure, and the mechanism by which the 3' end of the *pnd* mRNA inhibited translation remained enigmatic (Nielsen and Gerdes, 1995). The striking observation that the *tac* and *fbi* mutations in both *hok* and *pnd* mRNAs had similar dramatic effects on the RNA processing patterns caused us to investigate whether the ends of the mRNAs interact. The genetic data presented in Figs 3 and 4 show that this is the case. The precise pairing of the mRNA ends leads to blunt-ended intramolecular RNA duplexes in which the first nucleotides pair with the last nucleotides. These observations allow the formulation of secondary structure models of *hok* and *pnd* mRNAs that take into account information from both structural and genetic analyses. The deduced secondary structure of the entire full-length *hok* mRNA is shown in Fig. 2A.

The secondary structure model of the entire full-length *pnd* mRNA is presented in Fig. 2C, and was based on computer analysis, genetic data, and a comparison with the secondary structure model of the *hok* mRNA. The genetic data obtained by Nielsen and Gerdes (1995) showed that the *pndC* SD element is sequestered by a local upstream anti-SD element (Fig. 2C). By inference, we propose that the *hok* mRNA contains a similar anti-SD element, as indicated in Fig. 2A. This proposal is consistent with the structure-probing results of Thisted *et al.* (1995). In addition, the data presented in this study exclude the presence of a direct interaction between the extreme 3' end of the *hok* mRNA and the *mok* SD region as proposed by Thisted *et al.* (1995).

Killer mRNA translation occurs in plasmid-free cells and after the addition of rifampicin. This is understandable, as

the inhibitory Sok and PndB antisense RNAs are absent in plasmid-free cells. However, translation in plasmid-free cells (and after the addition of rifampicin) is dependent on the accumulation of an activatable pool of killer mRNA that has not yet reacted with its cognate antisense RNA (Gerdes *et al.*, 1992; Thisted *et al.*, 1994a; Nielsen and Gerdes, 1995). This is because inhibition by the antisense RNAs leads to RNA duplex formation, followed by irreversible inactivation of the duplexed RNAs by RNase III cleavage (Gerdes *et al.*, 1992). We have previously shown that the killer mRNAs possess the following three features, all of which are prerequisites for the induction mechanism: (i) the processing rates of full-length to truncated mRNAs are low; this is required because rapid truncation leads to depletion of the activatable pool of mRNA (Nielsen and Gerdes, 1995). (ii) The binding of the antisense RNAs to the full-length mRNAs is negligible (Thisted *et al.*, 1994b: T. Franch, unpublished); rapid antisense RNA binding would lead to duplex formation and irreversible inactivation by RNase III cleavage of the duplex (Gerdes *et al.*, 1992). (iii) The full-length mRNAs are translationally inactive (Gerdes *et al.*, 1990b; Nielsen *et al.*, 1991; Thisted *et al.*, 1994a): translation of the full-length mRNAs in plasmid-carrying cells would inadvertently result in cell killing.

The secondary structures of the full-length *hok* and *pnd* mRNAs proposed here explain all of the above observations. First. mutations that disrupt the pairing of the ends of the mRNA lead to increased processing, depletion of the mRNA pool, and inactivation of post-segregational killing (Figs 3 and 4; Table 1). Thus, the *fbi–tac* interaction maintains the required, low rate of the 3' processing of the full-length mRNAs. Second, full-length *hok* mRNA binds Sok RNA at an approx. 100-fold lower rate than its truncated version *in vivo* and *in vitro* (T. Franch, unpublished), indicating sequestration of the antisense RNA target in *hok* (and *pnd*) mRNA by the fold-back structure. Indeed, the antisense RNA target elements. denoted *sokT* and *pndBT*, are sequestered in the secondary structure models proposed in Fig. 2A and 2C. Third, the *fbi* element represses translation by sequestration of *tac*. In conclusion, the folded structures of the full-length *hok* and *pnd* mRNAs explain how they simultaneously avoid translation, antisense RNA binding, and rapid inactivation by 3' exonucleases.

The refolding model

The introduction of the *tac* mutations did not lead to functional suppression of the *fbi* mutations (Table 1). This was surprising, as the doubly mutated mRNAs exhibited normal processing patterns (Figs 3 and 4, panels D). This observation encouraged us to investigate the effect of the *tac* mutations on translation of truncated *hok* and *pnd* mRNAs. Surprisingly, introduction of mutations in

the *tac* elements, which are located approx. 100 nt upstream of the *mok* and *pndC* reading frames, severely impaired translation (Fig. 5). Furthermore, analysis of deletions and substitutions in *tac* firmly established that *tac* is indeed required for translation (Fig. 6).

The mechanism by which *tac* activates translation is not yet known. However, the *tac* elements are complementary to the anti-SD elements (see Fig. 2, B and D). This suggests that the exonucleolytical removal of the *fbi* elements triggers the *tac* elements to base pair instead with the anti-SD elements. Computer analyses using the 'genetic algorithm' developed by Gultyaev *et al.* (1995) corroborated this suggestion (Alexander P. Gultyaev, T. Franch and K. Gerdes, unpublished). The proposed secondary structures of the refolded forms of the truncated wt *hok* and *pnd* mRNAs are shown in Fig. 2, B and D. In these structures, the *tac* sequences pair with the anti-SD sequences, thus releasing the *mok* and *pndC* SD regions into configurations that are more accessible for ribosome binding. The proposed refolding pathway is particularly attractive because it does not require the formation of energetically unfavourable folding intermediates, but rather could occur by a branch-migration-like mechanism in which the *tac* elements gradually form successive base pairs with the anti-SD elements, while breaking base pairs in the lower part of the *pndC*-SD/*mok*-SD stem (see Fig. 2).

The refolding model predicts that mutational changes in *tac* that destabilize its pairing with the anti-SD sequences should lead to reduced translatability. The mutational analysis of *tac* presented in Fig. 6 concurs with this notion: those mutations in *tac* that most severely disrupted the potential base pairing with the anti-SD elements (*tac2*, *tacΔ7*, *tacΔ10* and *tac5A* in *hok*, and *tac552* in *pnd*) exhibited the lowest translation rates, whereas those which still allowed some base pairing (*tac8* and *tacΔ3* in *hok*) were all, to some extent, translatable. Furthermore, the *hok* mRNA with the perfect *tac* stem mutation was translated at least twofold more efficiently than the wt *hok* mRNA (Fig. 6). These results show that the degree of translatability of the *hok* (and *pnd*) mRNA is correlated with the strength of the *tac*–anti-SD interaction. Thus, our results support the refolding model. By accomplishing *in vitro* secondary structure analyses of wt and *tac*-mutated mRNAs, we have now obtained direct evidence for the postulated interaction between *tac* and the anti-SD element in *hok* mRNA (T. Franch, unpublished results).

It has not previously been shown that a processing event in the 3′ end of an mRNA activates a positive translational control element in its 5′ end. However, the translation initiation region of the bacteriophage λ *cIII* gene mRNA was postulated to exist in two configurations, one of which allowed translation (Altuvia *et al.*, 1989, 1991). RNase III was found to stimulate *cIII* mRNA translation, and indirect evidence was obtained that RNAse III binding (without

cleavage) trapped the *cIII* mRNA translation initiation region in a translatable configuration (Altuvia *et al.*, 1987; 1991). From previous work, we can exclude that RNase III is involved in *hok* and *pnd* translation, as activation occurs in RNase III-deficient cells (Gerdes *et al.*, 1992).

The presence of positively acting translational control elements located in mRNA 5′ ends have been described in a few additional cases. Translation of bacteriophage lambda *cII* mRNA requires integration host factor (Mahajna *et al.*, 1986). The mRNA of the *cob* operon of *Salmonella typhimurium* contains an upstream element which prevents the inhibitory effect of a local secondary structure surrounding the *cbiA* SD element (Richter-Dahlfors *et al.*, 1994). The mechanism of action of the upstream element is unknown. The coat protein mRNA of bacteriophage MS2 contains a positively acting element located several-hundred nucleotides upstream of the translational start site (Kastelein *et al.*, 1983). This element counteracts the inhibition by a local stem-loop structure, which sequesters the SD region of the coat-protein cistron (de Smit and van Duin, 1993). However, its mechanism of action remains to be clarified. Finally, positively acting elements have been found in the 5′ untranslated regions in a number of mRNAs from chloroplasts (Sakamoto *et al.*, 1994).

The work presented in this study provides evidence that the highly folded structures of a class of prokaryotic mRNAs involve pairing of the ends of the mRNAs. The pairing explains the molecular mechanism underlying activation of killer mRNA translation in plasmid-free cells and after the addition of rifampicin.

Experimental procedures

Enzymes and chemicals

Rifampicin (Ciba-Geigy) was added to cells prior to RNA extraction at a concentration of 100 μg ml^{-1}. Ampicillin (Ap) was added at the following concentration: 30 μg ml^{-1} for low-copy-number plasmids, otherwise 100 μg ml^{-1}. All enzymes were purchased from Boehringer Mannheim unless stated otherwise.

Bacterial strains and plasmids

The *E. coli* K-12 strain CSH50 (Δ(*lac pro*) *rpsL*) (Miller, 1972) was used for the plasmid stability tests, whereas the permeable *E. coli* B strain AS19 (Sekiguchi and Iida, 1967) was used in the rifampicin induction experiments.

Plasmids used and constructed are listed in Table 2. Plasmid pPR633 carries the 580 bp wt *hok/sok* system from plasmid R1 cloned between the *Eco*RI–*Bam*HI sites of pBR322. Plasmids pTF40 (*tac2*), pTF41 (*fbi2*), pTF42 (*tac2*–*fbi2*), pTF50 (*tac8*), pTF51 (*fbi8*) and pTF52 (*tac8*–*fbi8*) are all mutant derivatives of pPR633. Plasmid pTT820 carries the 580 bp wt *hok/sok* system inserted between the *Eco*RI–*Bam*HI sites of the mini-R1 vector pOU82. Plasmids pTF840

Table 2. Plasmids used in this study.

Plasmid	Type of replicon	Relevant genotypes	Killer system present	Mutations[a]	Source/Reference
PUC19	pMB1	*bla⁺*	None	–	Yanisch-Perron *et al.* (1985)
pBR322	pMB1	*bla⁻ tet'*	None	–	Bolivar *et al.* (1977)
pBR633	pBR322	*bla⁻*	*hok/sok*	wt	Rasmussen *et al.* (1987)
pGEM342	pGEM4	*bla⁺* pT7	pPROBE*hok*	–	Thisted and Gerdes (1992)
pAN7	pGEM4	*bla⁻* pT7	pPROBE*pnd*	–	Nielsen *et al.* (1991)
pTF40	pBR322	*bla⁻*	*hok/sok*	*tac2*	This work
pTF41	pBR322	*bla⁻*	*hok/sok*	*fbi2*	This work
pTF42	pBR322	*bla⁻*	*hok/sok*	*tac2, fbi2*	This work
pTF60	pBR322	*bla⁻*	*hok/sok*	*tac8*	This work
pTF51	pBR322	*bla⁻*	*hok/sok*	*fbi8*	This work
pTF52	pBR322	*bla⁻*	*hok/sok*	*tac8, fbi8*	This work
pAN1	pBR322	*bla⁻*	*pnd*	wt	Nielsen *et al.* (1991)
pKG39	pBR322	*bla⁻*	*pnd*	*tac552*	This work
pAN41	pBR322	*bla⁻*	*pnd*	*fbi552*	Nielsen and Gerdes (1995)
pKG40	pBR322	*bla⁻*	*pnd*	*tac552, fbi552*	This work
pOU82	R1	*bla⁻ lac⁻*	None	–	Dam and Gerdes (1994)
pTF840	R1	*bla⁻ lac⁻*	*hok/sok*	*tac2*	This work
pTF841	R1	*bla⁻ lac⁻*	*hok/sok*	*fbi2*	This work
pTF842	R1	*bla⁻ lac⁻*	*hok/sok*	*tac2, fbi2*	This work
pTF850	R1	*bla⁻ lac⁻*	*hok/sok*	*tac8*	This work
pTF851	R1	*bla⁻ lac⁻*	*hok/sok*	*fbi8*	This work
pTF852	R1	*bla⁻ lac⁻*	*hok/sok*	*tac8, fbi8*	This work
pTT820	R1	*bla⁻ lac⁻*	*hok/sok*	wt	Thisted and Gerdes (1992)
pAN3	R1	*bla⁻ lac⁻*	*pnd*	wt	Gerdes *et al.* (1992)
pKG860	R1	*bla⁻ lac⁻*	*pnd*	*tac552*	This work
pAN141	R1	*bla⁻ lac⁻*	*pnd*	*fbi552*	Nielsen and Gerdes (1995)
pKG862	R1	*bla⁻ lac⁻*	*pnd*	*tac552, fbi552*	This work

a. The base changes of the *tac* and *fbi* mutations are shown in Figs 2 and 6.

(*tac2*), pTF841 (*fbi2*), pTF842 (*tac2–fbi2*). pTF850 (*tac8*), pTF851 (*fbi8*) and pTF852 (*tac8–fbi8*) are all mutant derivatives of pTT820.

Plasmid pAN1 carries the 856 bp wt *pnd* system from plasmid R483 cloned between the *Eco*RI–*Bam*HI sites of pBR322. Plasmids pKG39 (*tac552*), pAN41 (*fbi552*) and pKG40 (*tac552–fbi552*) are all mutant derivatives of pAN1. Plasmid pAN3 carries the 856 bp wt *pnd* system inserted between the *Eco*RI–*Bam*HI sites of pOU82. Plasmids pKG860 (*tac552*), pAN141 (*fbi552*) and pKG862 (*tac552–fbi552*) are mutant derivatives of pAN3.

Site-directed mutagenesis

The *tac2, tac2–fbi2, tac8, fbi8* and *tac8–fbi8* mutants were constructed by double polymerase chain reaction (PCR) as described by Barettino *et al.* (1994). The first round of PCR was performed using the M13mp18 vector carrying the 580 bp wt *hok/sok* system inserted between the *Eco*RI–*Bam*HI sites as template. Either the reverse sequencing primer (5'-AACGCTATGACCATG-3') or the −20 sequencing primer (5'-GTAAAACGACGGCCAGT-3') were used as external primers. In the second round of PCR, the plasmids pPR633, pTF41 (for *tac2–fbi2* construction) or pTF51 (for *tac8–fbi8* construction) were used as templates. Either counter-clockwise *Bam*HI (5'-CACGATGCGTCCGGCGTAG-3') or clockwise *Eco*RI (5'-GTATCACGAGGCCCTTTCG-3') were used as external primers. Mutant oligonucleotides used were: TF4 (*tac2*) 5'-AAGCCTCAAGCGGGGGGCACATCATA-3', TF5 (*tac8*) 5'-AAAGCCTCAAGCCGCGGGCACATCAT-3' and

TF6 (*fbi8*) 5'-GACTACTGAAGCCGCTTTATAAAGGGG-3' (mutated nucleotides are underlined). The construction of pTF41 (previously termed pPR633*fbi2*) was described by Thisted *et al.* (1995).

Introduction of mutations in the *pnd* system was accomplished by double PCR using two complementary mutant oligonucleotides and two external primers as described by Nielsen and Gerdes (1995). Mutant oligonucleotides used were: pnd174B (*tac552a*) 5'-GCCTCAAGCGGGCGCAGC-TATTC-3' and pnd196 (*tac552b*) 5'-GAATAGCTGCGCC-CGCTTGAGGC-3'. External primers were: pnd21 5'-GG-GGATCCTGCGACAGGCTGTCGATTGT-3' (*Bam*HI overhang) and pnd611 5'-GGGAATTCGCAAAGGCATTCGGC-TGGAG-3' (*Eco*RI overhang). For the construction of *tac552*, PCR was conducted using a wt *pnd* template, while the *tac552–fbi552* mutant was constructed by PCR on the pAN41 template. For the construction of *fbi552*, see Nielsen and Gerdes (1995).

Measurement of plasmid stability

Plasmid stability tests were performed as described in Gerdes *et al.* (1985).

Total RNA preparation for Northern transfer analysis

Preparation of total RNA from *E. coli* and Northern transfer analysis was performed as described earlier (Gerdes *et al.*, 1990b). The ^{32}P-labelled RNA probes used were generated using T7 RNA polymerase and the pGEM-based plasmids

pGEM342 (*hok* probe) and pAN7 (*pnd* probe), as described previously (Gerdes *et al.*, 1990b; Nielsen *et al.*, 1991).

Preparation of hok and pnd mRNAs

Large scale wt and mutant *in vitro* synthesized *hok* and *pnd* transcripts of different lengths were synthesized using T7 RNA polymerase and DNA templates generated by PCR (Thisted *et al.*, 1994a). In the PCR reactions, the T7-1 oligo-nucleotide or a mutated analogous oligonucleotide comple-mentary to +1 to +24 in the *hok/sok* system and containing the T7 promoter sequence, was used as the upstream oligo-nucleotide. The second oligonucleotide specified the length of the PCR DNA fragment, thus determining the 3′ end of the RNA run-off transcript synthesized by T7 RNA polymerase: T7-1, 5′-CGGGATCCTGTAATACGACTCACTATAGGCGCT-TGAGGCTTTCTCCTCATG-3′ (sequence complementary to *hok/sok* is underlined); T7-4, 5′-AAGGCGCTTCAGTAGT-CAG-3′ (results in a run-off transcript with the 3′ end at +398, corresponding to *hok* mRNA-2); T7-3N, 5′-AAGGC-GGGCCTGCGCCCGCCTCCAGG-3′ (run-off transcript with 3′ end at +361, corresponding to truncated *hok* mRNA).

DNA templates containing T7 promoter sequences used for synthesis of *pnd* transcripts were generated in a similar fash-ion using the oligonucleotides: T7-AN, 5′-CGGGATCCTG-TAATACGACTCACTATAGGGCGCTTGAGGCTGTATGCC-GAA-3′ (the sequence complementary to *pnd* from +1 to +24 is underlined); AN5, 5′-GGGCGAATGAGGTCAGCC-TTCGCAAC-3′ (results in a run-off transcript with a 3′ end at +371, corresponding to full-length *pnd* mRNA); AN2B, 5′-GCGGCGGCAGAAAACCTGCCGCCG-3′ (results in a run-off transcript with a 3′ end at +341, corresponding to truncated *pnd* mRNA). *In vitro* synthesis of mutated *hok* and *pnd* mRNAs was accomplished as described above, except that the oligonucleotides used carried the relevant nucleotide substitutions, as shown in Fig. 6.

The DNA fragment amplified by PCR was recovered from an agarose gel, phenol–chloroform extracted, precipitated and resuspended in H_2O, and finally transcribed *in vitro* with T7 RNA polymerase. Unlabelled transcripts ([^{3}H]-CTP) were synthesized in a 100 μl reaction of the following composition: 40 mM Tris-HCl, pH 7.5, 2 mM spermidine, 10 mM NaCl, 24 mM $MgCl_2$, 6.4 μM [^{3}H]-CTP (NEN), 4.0 mM each of ATP, GTP, UTP and CTP, 10 mM dithiothreitol (DTT), 160 U RNasin (Promega), 50 U T7 RNA polymerase (Promega) and approx. 3–5 μg DNA template. Transcription was performed overnight at 37°C. Labelled transcripts ([^{32}P]-CTP) were synthesized in a 50 μl reaction with the following composition: 40 mM Tris-HCl, pH 7.5, 2 mM spermidine, 10 mM NaCl, 6 mM $MgCl_2$, 10 mM DTT, 0.5 mM each of ATP, UTP and GTP, 40 μM CTP, 0.5 μM [^{32}P]-CTP (NEN), 60 U RNasin (Promega), 30 U T7 RNA polymerase (Promega) and approx. 1–2 μg of DNA template. The reactions were incubated for 2 h at 37°C

Transcript recovery was accomplished as described in Persson *et al.* (1988). Transcripts were fractionated on gels of 5.5% acrylamide and 8 M urea. The transcripts were eluted from the gels by soaking the crushed gel slices at 20°C for 60 min in 500 μl of elution buffer (0.1 M NaOAc, pH 5.7, 10 mM Na_2EDTA, 0.5% SDS) containing 6 μg of carrier tRNA. Gel debris was removed by centrifugation. Transcripts

were phenol–chloroform extracted, precipitated twice with ethanol, washed and dried. After gel purification, transcripts were redissolved in TE buffer.

Test of transcript stability in the E. coli S30 extract

Uniformly ^{32}P-labelled transcripts were incubated at 37°C in an *E. coli* S30 extract under similar conditions as for the *in vitro* translation reactions described below, except that the [^{35}S]-methionine was replaced by unlabelled methionine. Samples were withdrawn and immediately phenol–chloroform extracted, run on 5.5% acrylamide gels, which were dried down and autoradiographed.

In vitro translations and SDS–PAGE

The *E. coli* coupled transcription/translation system (Zubay, 1973) was purchased from Promega. The translation reac-tions contained the following components in a total volume of 20 μl: 3 pmol ^{3}H-labelled *hok* or *pnd* mRNA in 5 μl TE, 0.5 mM each of the 20 amino acids, minus methionine, 0.2 μM ʟ-[^{35}S]-methionine (1000 Ci mmol^{-1}; NEN), 2 mM ATP, 0.5 mM each of GTP, UTP, and CTP, 210 mM potassium glutamate, 20 mM PEP, 35 mM Tris-OAc, pH 8.0, 27 mM NH_4OAc, 1 mM cAMP, 20 μg ml^{-1} folinic acid, 100 μg ml^{-1} *E. coli* tRNA, 9 mM Mg(OAc)$_2$, 0.8 mM IPTG, 2 mM DTT, 35 mg ml^{-1} PEG 8000, and 6 μl *E. coli* S30 extract. In the translations shown in Fig. 5, the reactions were allowed to pro-ceed for 30 min. The samples were precipitated with four volumes of acetone at 0°C, dried and redissolved in 2 × SDS sample buffer (per 10 ml: 2 ml glycerol, 2 ml 10% SDS, 0.25 mg bromophenol blue, 2.5 ml of 0.5 mM Tris-HCl, pH 6.8, in 0.4% SDS, 0.5 ml β-mercaptoethanol) and denatured at 100°C for 5 min prior to loading onto SDS gels. For optimal resolution of the low-molecular-mass proteins (5–20 kDa), the discontinuous tricine–SDS–PAGE system described by Schägger (1985) was used. The stacking gel contained 4% acrylamide and the separation gel 16% acrylamide. Electro-phoresis was carried out at 30 V in the stacking gel, and when the sample had reached the separation gel the current was increased to 25 mA for the remainder of the run (total run-ning time was approx. 20 h). The gel was fixed in a solution of 50% methanol, 20% acetic acid and 10% glycerol for 1 h, and then washed in a solution of 25% ethanol and 5% acetic acid.

References

Altuvia, S., Locker-Giladi, H., Koby, S., Ben-Nun, O., and Oppenheim, A.B. (1987) RNase III stimulates the transla-tion of the *cIII* gene of bacteriophage lambda. *Proc Natl Acad Sci USA* 84: 6511–6515.

Altuvia, S., Kornitzer, D., Teff, D., and Oppenheim, B. (1989) Alternative mRNA structures of the *cIII* gene of bacteriophage I determine the rate of its translation initiation. *J Mol Biol* 210: 265–280.

Altuvia, S., Kornitzer, D., Kobi, S., and Oppenheim, B. (1991) Functional and structural elements of the mRNA of the *cIII* gene of bacteriophage lambda. *J Mol Biol* 218: 723–733.

Barettino, D., Feigenbutz, M., Valcárcel, R., Stunnenberg, H.G. (1994) Improved method for PCR-mediated site-directed mutagenesis. *Nucl Acids Res* 22: 541–542.

Bolivar, F., Rodriquez, R.L., Greene, P.J., Betlach, M.C., Heyneker, H.L., Boyer, H.W., Crosa, J.H., and Falkow, S. (1977) Construction and characterization of new cloning vehicles. II. A multipurpose cloning system. *Gene* 2: 95–113.

Dam, M., and Gerdes, K. (1994) Partitioning of plasmid R1: 10 direct repeats flanking the *parA* promoter constitute a centromere-like partition site, *parC*, that expresses incompatibility. *J Mol Biol* 236: 1289–1298.

Eguchi, Y., Itoh, T., and Tomizawa, J. (1991) Antisense RNA. *Annu Rev Biochem* 60: 631–652.

Gerdes, K., Larsen, J.E.L., and Molin, S. (1985) Stable inheritance of plasmid R1 requires two different loci. *J Bacteriol* 161: 292–298.

Gerdes, K., Rasmussen, P.B., and Molin, S. (1986a) Unique type of plasmid maintenance function: postsegregational killing of plasmid-free cells. *Proc Natl Acad Sci USA* 83: 3116–3120.

Gerdes, K., Bech, F.W., Jorgensen, S.T., Lobner-Olesen, A., Atlung, T., Boe, L., Karlstrom, O., Molin, S., and von Meyenburg, K. (1986b) Mechanism of postsegregational killing by the *hok* gene product of the *parB* system of plasmid R1 and its homology with the *relF* gene product of the *E. coli relB* operon. *EMBO J.* 5: 2023–2029.

Gerdes, K., Helin, K., Christensen, O.W., and Løbner-Olesen, A. (1988) Translational control and differential RNA decay are key elements regulating postsegregational expression of the killer protein encoded by the *parB* locus of plasmid R. *Mol Biol* 203: 119–129.

Gerdes, K., Poulsen, L.K., Thisted, T., Nielsen, A.K., Martinussen, J., and Hove-Andreasen, P. (1990a) The *hok* killer gene family in Gram-negative bacteria. *New Biologist* 2: 946–956.

Gerdes, K., Thisted, T., and Martinussen, J. (1990b) Mechanism of post-segregational killing by the *hok/sok* system of plasmid R1: the *sok* anti-sense RNA regulates the formation of a *hok* mRNA species correlated with killing of plasmid-free cells. *Mol Microbiol* 4: 1807–1818.

Gerdes, K., Nielsen, A., Thorsted, P., and Wagner, E.G.H. (1992) Mechanism of killer gene reactivation: antisense RNA mediated RNase III cleavage ensures rapid turn-over of the *hok*, *srnB* and *pndA* effector mRNAs. *J Mol Biol* 226: 637–649.

Gold, L. (1988) Posttranscriptional regulatory mechanisms in *Escherichia coli*. *Ann Rev Biochem* 57: 199–233.

Gultyaev, A.P., van Batenburg, F.H.D., and Pleij, C.W.A. (1995) The computer simulation of RNA folding pathways using a genetic algorithm. *J Mol Biol* 250: 37–51.

Kastelein, R.A., Berkhout, B., Overbeek, G.P., and van Duin, J. (1983) Effect of the sequences from the ribosome-binding site on the yield of protein from the cloned gene for phage MS2 coat protein. *Gene* 23: 245–254.

McCarthy, J.E.G., and Gualerzi, C. (1990) Translational control of prokaryotic gene expression. *Trends Genet* 3: 78–85.

McCarthy, J.E.G., and Brimacombe, R. (1994) Prokaryotic translation: the interactive pathway leading to initiation. *Trends Genet* 10: 402–407.

Mahajna, J., Oppenheim, A.B., Rattray, A., and Gottesman, M. (1986) Translation initiation of bacteriophage lambda *cII* requires integration host factor. *J Bacteriol* 165: 167–174.

Miller, J. (1972) *Experiments in Molecular Genetics*. Cold Spring Harbor, New York: Cold Spring Harbor Laboratory Press.

Nielsen, A.K., and Gerdes, K. (1995) Mechanism of post-segregational killing by *hok*-homologue *pnd* of plasmid R483: two translational control elements in the *pnd* mRNA. *J Mol Biol* 249: 270–282.

Nielsen, A.K., Thorsted, P., Wagner, E.G.H., and Gerdes, K. (1991) The rifampicin inducible genes *srnB* from F and *pnd* from R483 are regulated by antisense RNAs and mediate plasmid maintenance by killing of plasmid-free segregants. *Mol Microbiol* 5: 1961–1973.

Persson, C., Wagner, E.G.H., and Nordström, K. (1988) Control of replication of plasmid R1: kinetics of *in vitro* interaction between the antisense RNA, CopA, and its target, CopT. *EMBO J* 7: 3279–3288.

Petersen, C. (1989) Long range translational coupling in the *rplJL–rpoBC* operon of *Escherichia coli*. *J Mol Biol* 206: 323–332.

Poulsen, L.K., Refn, A., Molin, S., and Andersson, P. (1991) A family of genes encoding a cell-killing function may be conserved in all Gram-negative bacteria. *Mol Microbiol* 3: 1463–1472.

Rasmussen, P.B., Gerdes, K., and Molin, S. (1987) Genetic analysis of the *parB* locus of plasmid R1. (1987) *Mol Gen Genet* 209: 122–128.

Richter-Dahlfors, A.A., Ravnum, S., and Andersson, D.I. (1994) Vitamin B12 represssion of the *cob* operon in *Salmonella typhimurium*: translational control of the *cbiA* gene. *Mol Microbiol* 13: 541–553.

Saito, H., and Richardson, C.C. (1981) Processing of mRNA by ribonuclease III regulates expression of gene 1.2 of bacteriophage T7. *Cell* 27: 533–542.

Sakamoto, W., Chen, X., Kindle, K.L., Stern, D.B. (1994) Function of the *Chlamydomonas reinhardtii petD* 5' untranslated region in regulating the accumulation of subunit IV of the cytochrome 6/f complex. *Plant J* 6: 503–512.

Schägger, H., Borchart, U., Aquila, H., Link, T.A., and von Jagow, G. (1985) Isolation and amino acid sequence of the smallest subunit of beef heart Bcl complex. *FEBS Lett* 190: 89–94.

Sekiguchi, M., and Iida, S. (1967) Mutants of *Escherichia coli* permeable to actinomycin. *Proc Natl Acad Sci USA* 58: 2315–2320.

de Smit, M., and van Duin, J. (1990) Control of prokaryotic translation initiation by mRNA secondary structure. *Prog Nucleic Acid Res Mol Biol* 38: 1–35.

de Smit, M., and van Duin, J. (1993) Translational initiation of

the coat-protein gene of phage MS2: native upstream RNA relieves inhibition by local secondary structure. *Mol Microbiol* 9: 1079–1088.

Thisted, T., and Gerdes, K. (1992) Mechanism of post-segregational killing by the *hok/sok* system of plasmid R1: *sok* antisense RNA regulates *hok* gene expression indirectly through the overlapping *mok* reading frame. *J Mol Biol* 223: 41–54.

Thisted, T., Nielsen, A.K., and Gerdes, K. (1994a) Mechanism of post-segregational killing: translation of *hok*, *srnB* and *pnd* mRNAs of plasmids R1, F and R483 is activated by 3′-end processing. *EMBO J* 13: 1950–1959.

Thisted, T., Sørensen, N.S., Wagner, E.G.H., and Gerdes, K. (1994b) Mechanism of post-segregational killing: *sok* antisense RNA interacts with *hok* mRNA via its 5′-end single-stranded leader and competes with the 3′-end of *hok*

mRNA for binding to the *mok* translational initiation region. *EMBO J* 13: 1960–1968.

Thisted, T., Sørensen, N.S., and Gerdes, K. (1995) Mechanism of postsegregational killing: secondary structure analysis of the entire *hok* mRNA from plasmid R1 suggests a fold-back structure that prevents translation and antisense RNA binding. *J Mol Biol* 247: 859–873.

Wagner, E.G.H., and Simons, R.W. (1994) Antisense RNA control in bacteria, phages and plasmids. *Annu Rev Microbiol* 48: 713–742.

Yanisch-Perron, C., Vieira, J., and Messing, J. (1985) Improved M13 phage cloning vectors and host strains: nucleotide sequences of the M13mp18 and pUC19 vectors. *Gene* 33: 103–109.

Zubay, G. (1973) *In vitro* synthesis of protein in microbial systems. *Annu Rev Genet* 7: 267–287.